

# Auto-Agent-Distiller: Towards Efficient Deep Reinforcement Learning Agents via Neural Architecture Search

Yonggan Fu  
Rice University  
yf22@rice.edu

Zhongzhi Yu  
Rice University  
zy42@rice.edu

Yongan Zhang  
Rice University  
yz87@rice.edu

Yingyan Lin  
Rice University  
yingyan.lin@rice.edu

## Abstract

*AlphaGo’s astonishing performance has ignited an explosive interest in developing deep reinforcement learning (DRL) for numerous real-world applications, such as intelligent robotics. However, the often prohibitive complexity of DRL stands at the odds with the required real-time control and constrained resources in many DRL applications, limiting the great potential of DRL powered intelligent devices. While substantial efforts have been devoted to compressing other deep learning models, existing works barely touch the surface of compressing DRL. In this work, we first identify that there exists an optimal model size of DRL that can maximize both the test scores and efficiency, motivating the need for task-specific DRL agents. We therefore propose an Auto-Agent-Distiller (A2D) framework, which to our best knowledge is the first neural architecture search (NAS) applied to DRL to automatically search for the optimal DRL agents for various tasks that optimize both the test scores and efficiency. Specifically, we demonstrate that vanilla NAS can easily fail in searching for the optimal agents, due to its resulting high variance in DRL training stability, and then develop a novel distillation mechanism to distill the knowledge from both the teacher agent’s actor and critic to stabilize the searching process and improve the searched agents’ optimality. Extensive experiments and ablation studies consistently validate our findings and the advantages and general applicability of our A2D, outperforming manually designed DRL in both the test scores and efficiency. All the codes will be released upon acceptance.*

## 1. Introduction

Deep reinforcement learning (DRL) [48] which integrates reinforcement learning (RL) and deep neural networks (DNNs) has dramatically broadened the range of complex decision-making tasks that were previously outside of the capability of machines. In particular, DRL opens up the possibility to mimic some human problem solving capabilities in high-dimensional space thanks to its capabil-

ity to learn different levels of abstractions from data even with lower prior knowledge. Recent successes of DRL agents, such as beating the world-champion Go grandmaster equipped in Google’s AlphaGo and beating human video game players, have triggered tremendously increased enthusiasm to develop and deploy DRL-powered intelligence into numerous real-world inference and control applications, including robotics [42, 22, 53], autonomous vehicles [83], finance [15] and smart grids [19]. Many of these applications, such as autonomous vehicles, require real-time control and decision-making policies for which the DRL agents have to derive real-time policies using real-time data for dynamic systems, i.e., the policy inference must be done in real-time at the control frequency of the system, which for example is on the order of milliseconds for a recommender system [12] responding to a user request. However, real-time control and decision-making for DRL can be prohibitively challenging in many real-world applications due to DRL’s integrated complex DNNs and edge devices’ constrained resources, calling for DRL agent designs that favor both test score and processing efficiency.

In parallel, most existing DRL works adopt a fixed DNN backbone for the agent without explicitly exploring the relationship between the agents’ model sizes and DRL’s achieved test scores, let alone the test score and processing efficiency trade-off. While one can naturally think that increasing the model size in general will benefit the test score as commonly observed in visual classification tasks [69], we empirically find that there exists a task-specific optimal model size for DRL’s DNN agents that maximizes the achieved test score, from which further increasing the model sizes will not improve or even hurt the performance which we conjecture is due to the increased training difficulty of more complex DRL agents. This indicates that the DNN architecture for DRL agents has to balance both its model capability and imposed difficulty to DRL training, which can be very different for diverse DRL applications with different specification and task difficulty. Thus, task-specific DRL agent designs are highly desired to facilitate the development of optimal DRL-powered solutions

that maximize both DRL’s test scores and efficiency.

To close the aforementioned gap, neural architecture search (NAS) [86, 87, 45] is a promising solution as it can automate the agent design without the need for laboriously huge human efforts for each task, motivated by the recent success of AutoML [35]. However, directly applying NAS to design DRL agents can easily fail due to the commonly observed vulnerability and instability of DRL training, which occurs with a high variance as discussed in [11, 29, 1, 56], making it difficult to correctly rank the sampled networks within a limited search time. Furthermore, such an instability will be further exacerbated when considering differentiable NAS (DNAS), which has the advantage of competitively low search cost and thus favors the fast development of DRL-powered solutions, because the success of DNAS requires unbiased gradient estimation with a low variance. To this end, we aim to develop a novel and effective NAS framework dedicated to DRL agent designs to promote fast development and high-quality DRL-powered intelligent solutions for numerous applications. Specifically, we make the following contributions:

- We identify that there exists an optimal model size for DRL agents that maximize both the test scores and efficiency for each task, motivating task-specific DRL agent designs and calling for fast and automated DRL agent design techniques to address the growing demand for DRL-powered intelligent real-world devices.
- We propose an Auto-Agent-Distiller (A2D) framework, which to our best knowledge is the first NAS dedicated to DRL, aiming to automatically and efficiently search for the optimal network architectures for DRL’s DNN agents on different tasks. The effectiveness of A2D is attributed to a novel distillation mechanism on top of the state-of-the-art (SOTA) DRL using Actor-Critic (AC) methods, effectively stabilizing the NAS search despite the instability of DRL training.
- Extensive experiments and ablation studies consistently validate our findings and the superiority and general applicability of our A2D, largely outperforming existing DRL in both the test scores and efficiency. We believe this work has enhanced our understanding in NAS for DRL agent design and could open up the possibility of automated and fast development of DRL-powered solutions for many real-world applications.

## 2. Related Works

### 2.1. Deep Reinforcement Learning

Traditional RL algorithms can be categorized into two groups: value-based and policy-based methods. Value-based methods [78, 57] aim to build a value function, which

subsequently allows the definition of a policy; and policy-based methods [67] directly model the policy to maximize the expected return in either a gradient-free [23, 13] or gradient-based way [67]. To take advantage of both methods, AC-based RL methods [40] try to combine both value-based and policy-based methods, in which an actor learns the feedback from a critic to trade-off both the variance introduced by policy-based methods and the bias introduced by value-based methods. Motivated by the recent success of DNNs, DRL integrates traditional RL algorithms with DNNs by approximating the optimal value function or policy using DNNs in order to scale up prior RL works to handle higher-dimensional and more complex problems. Specifically, along the value-based track, DQN [48] first introduces DNNs to Q-Learning [78], and later [77, 72, 60, 3, 18] further improve DQN towards better value estimation and [30] combines the previous efforts to demonstrate a strong baseline; Along the policy-based track, [62, 63, 46, 64] develop deep policy gradient methods on top of [67]; And along the AC track, [47, 76, 81, 17, 24] empower both the actor and critic using DNNs and [43, 2, 21] further extend DRL to handle continuous control. The readers are referred to [1] for more details about DRL.

Despite the promising success of recent DRL methods, a majority of them focus merely on improving existing algorithms, with the DNN designs for DRL agents being under-explored. We thus aim to study the scalability of DRL with model sizes and automate the network design for DRL agents to promote fast development of powerful and efficient DRL-powered solutions for numerous applications.

### 2.2. Knowledge Transfer in DRL

Since DRL can suffer from high sample complexity which limits its achieved performance due to the insufficient interactions with the environment, transfer learning in DRL has demonstrated to be crucial for the practical use of DRL, where external expertise knowledge is utilized to accelerate the learning process of DRL. For instance, reward shaping [50, 79, 16, 7, 74] leverages the expertise knowledge to reshape the reward distributions to steer the agent’s action selection and navigation towards the expected trajectories; [59, 84, 39, 31, 49, 38, 74] make use of external demonstrations from different sources such as human experts or near-optimal policy to achieve more efficient exploration. Motivated by the recent success of knowledge distillation [32] in visual classification tasks and model compression [54], policy distillation [58] has gained increased popularity in DRL, which transfers the teacher policy in a supervised manner by minimizing the divergence between the teacher policy and the student policy. More recently, [14, 61] further extend this idea to enable better sample efficiency and [51, 70] apply it to multi-task DRL. More information about transfer learning in DRL can be found in [85].

Built upon the prior arts, our A2D integrates a new distillation mechanism, which not only distills the policy knowledge from the teacher actor but also the knowledge of value estimation from the teacher critic towards much improved student agent, leading to an effective NAS framework dedicated to powerful and efficient DRL agent design.

### 2.3. Neural Architecture Search

NAS [86] is an exciting new field which aims to automate the network design for different tasks for achieving both competitive performances and efficiency. Specifically, RL based NAS [86, 87, 68, 33, 69] and evolutionary algorithm based NAS [52, 55] explore the search space and train each sampled network candidate from scratch, suffering from prohibitive search costs. Later, DNAS [45, 80, 75, 8, 82] is proposed to update the weight and architecture in a differentiable manner through supernet weight sharing, which can reduce the search time to several hours [65]. Motivated by the promising performance achieved by those NAS works, recent works have extended NAS to more tasks such as segmentation [44, 10], image enhancement [20, 41], and language modeling [9].

The success of NAS in various tasks promise their great potential to boost DRL solutions' performance and efficiency and to enable DRL to handle large-scale real-world problems. However, to our best knowledge, existing works have not yet explored the possibility of using NAS to search for DRL agents. The main challenge is DRL's notorious training instability with a high variance as discussed in [11, 29, 1, 56], which makes it difficult to correctly rank the sampled networks within a limited search time. Furthermore, although DNAS is promising in enabling fast development of powerful DRL solutions as it can best satisfy the need of fast generation and deployment of high-quality DRL agents on various tasks, the DRL's training instability often occurring with a high variance stands at odds with DNAS's requirement of accurate gradient estimation with a low variance. To this end, our A2D aims to close the aforementioned gap in a timely response to the growing need for more powerful and efficient DRL-powered solutions.

### 3. Preliminaries of DRL

In this section, we provide preliminaries of DRL during which we also set up our adopted notations.

We assume the usual RL design, and that RL can be formulated as a Markov Decision Process (MDP) characterized using a tuple  $(S, A, T, R, \gamma)$ , where  $S$  is the state space,  $A$  is the action space,  $T(s'|s, a)$  is the transition probability of ending up in state  $s'$  when executing the action  $a$  in the state  $s$ ,  $R$  is the reward function, and  $\gamma$  is a discount factor. The behaviour of an agent in the MDP can be formulated as a policy  $\pi(s_t, a_t) = p(a_t|s_t)$ , which defines the probability of executing the action  $a$  in the state  $s$ . In particular,

at each time step  $t$  with the corresponding state  $s_t \in S$ , the agent performs the action  $a_t \in A$  sampled from the policy  $\pi(s_t, a_t)$ , resulting in the state  $s_{t+1} \in S$  based on the transition probability  $T(s_{t+1}|s_t, a)$  and the reward  $r_t$ . Accordingly, the expected cumulative reward achieved by a policy  $\pi$  can be formulated as:

$$J(\pi) = \mathbb{E}_\pi \left[ \sum_{t=0}^H \gamma^t r_t \right] \quad (1)$$

where  $H$  is the time horizon and  $\gamma$  is the discount factor. In DRL, the policy is parameterized by  $\theta_\pi$ , i.e., the weights of the DNN agent, and the agent aims to learn an optimal policy to maximize the expected cumulative reward:

$$\theta_\pi^* = \arg \max_{\theta_\pi} J(\pi(\cdot|\theta_\pi)) \quad (2)$$

for which stochastic policy gradient methods [67] are widely adopted to optimize the policy and the gradient of the expected cumulative reward w.r.t. the policy parameters, i.e.,  $\nabla_{\theta_\pi} J(\pi(\cdot|\theta_\pi))$ , is given by:

$$\nabla_{\theta_\pi} J(\pi(\cdot|\theta_\pi)) = \mathbb{E}_\pi \left[ \sum_{t=0}^H \delta_t \nabla_{\theta_\pi} \log(\pi(a_t, s_t|\theta_\pi)) \right] \quad (3)$$

where there are different ways to design  $\delta_t$  and we adopt the temporal difference error (td-error) following [66] for reducing the variance of the policy gradients, i.e.:

$$\delta_t = r_t + \gamma V_\pi(s_{t+1}|\theta_v) - V_\pi(s_t|\theta_v) \quad (4)$$

where  $V_\pi(s) = \mathbb{E}_\pi \left[ \sum_{t=0}^H \gamma^t r_t | s_0 = s \right]$  is the value function which estimates the expected cumulative reward of the policy  $\pi$  starting from the initial state  $s$ .

Since the value function is also unknown, the AC-based methods [40] approximate the value function (i.e., the critic) with the learnable parameter  $\theta_v$  which can be modeled using the weights of a DNN, and the learning objective of  $\theta_v$  is to minimize the td-error of the estimated value between consecutive states, as formulated below:

$$\theta_v^* = \arg \min_{\theta_v} \mathbb{E}_\pi \left[ \sum_{t=0}^H \frac{1}{2} (r_t + \gamma V_\pi(s_{t+1}|\theta_v) - V_\pi(s_t|\theta_v))^2 \right] \quad (5)$$

Therefore, the actor and critic parameterized by  $\theta_\pi$  and  $\theta_v$ , respectively can be updated in an iterative way to guide the agent towards an optimal policy.

### 4. Motivating Findings and Proposed Methods

In this section, we first present two motivating observations that motivate our proposed A2D framework based

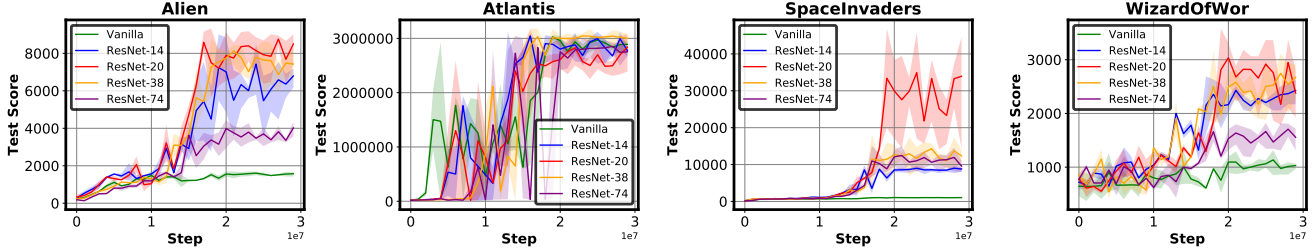


Figure 1. Test scores averaged over 30 episodes during the training of five models on four Atari games [4].

on experiments and discussions, i.e., the necessity of task-specific DRL agent designs in Sec. 4.1 and the failure of vanilla NAS in DRL in Sec. 4.2, and then introduce our proposed AC-based distillation mechanism and the A2D framework in Sec. 4.3 and Sec. 4.4, respectively.

#### 4.1. Finding 1: Scalability of DRL with Model Sizes

In this subsection, we provide experiments and discussions to show the need for task-specific DRL agent designs by studying the scalability of DRL with model sizes.

Most of existing DRL works adopt a fixed network backbone for the agents without explicitly studying the effect of model sizes to the final performance, leaving the scalability of DRL with model sizes unexplored and limiting the potential performance of DRL. To study this effect, we evaluate one of the most representative DRL, the AC-based DRL [40] method, when using various network backbones.

**Agent Backbone Design.** We follow the widely adopted network backbone design in existing AC-based DRL methods [17, 47], which uses a heavy feature extractor and two light-headers (implemented using two fully-connected layers) to design the actor and critic, respectively. Motivated by the success of SOTA DNN models, ResNet [27] series, as also demonstrated in recent DRL works [17], we adopt ResNets as the feature extractor, using the standard ResNet designed for the CIFAR-10 dataset [28], and scale up the model sizes by increasing its depth, during which we slightly modify the strides as well as the first and last layer of the networks to adapt the networks to the target DRL tasks as detailed in Appendix. C.

**Evaluation Settings.** Note that we use the same training and test hyper-parameters settings for all the models on all the tasks in this paper. Models and tasks: we evaluate the performance of the AC-based DRL when its feature extractor backbone adopts five different networks with different model sizes, including the original small network in DQN [48] (termed as the Vanilla), ResNet-14, ResNet-20, ResNet-38, and ResNet-74, on Atari 2600 games based on the Arcade Learning Environment [4]. Training settings: we train a DRL agent on each task for  $3e7$  steps with a discount factor ( $\gamma$  in Eq. 1) of 0.99 and a rollout length of 5. We use the RMSProp optimizer as [48] with an initial learning of  $1e-3$  which keeps constant in the first  $1e7$  steps and then linearly decays to  $1e-4$ . We adopt the standard loss for

Table 1. The best test scores achieved by different models on 15 Atari games. More results can be found in Appendix. A.

	Vanilla	ResNet-14	ResNet-20	ResNet-38	ResNet-74
Alien	1724	9007	<b>9323</b>	8829	4456
Amidar	721.8	638.6	<b>845.2</b>	138.3	493.9
Assault	10164	14470	<b>17314</b>	12406.5	9849
Asterix	4850	708500	<b>856800</b>	756120	539060
Asteroids	2095	5690	<b>5744</b>	1947	4792
BankHeist	1152	<b>1288</b>	1284	981	1163
BattleZone	7600	5800	13100	<b>13300</b>	4100
BeamRider	5530	23984	25961	29498	<b>30048</b>
Boxing	4.2	<b>100</b>	<b>100</b>	99.3	87.1
ChopperCommand	1320	11170	<b>14910</b>	4370	8240
DemonAttack	318349	481818	484382	<b>494569</b>	448450
Pong	-19.9	<b>21</b>	20.9	20.9	20.8
SpaceInvaders	1171	9848	<b>46870</b>	17962	15111
Tennis	-23.7	13.8	11.5	<b>19.6</b>	19.3
WizardOfWor	1320	2690	<b>3580</b>	3160	1850

the actor and critic as in Eq. 2 and Eq. 5 as well as an entropy loss on top of the actor to encourage exploration as in [24]. Test settings: the reported test score is averaged on 30 episodes with null-op starts following [48].

**Observations and Analysis.** We visualize the test score evolution during the training process on various Atari games, when adopting different networks for the DRL agents as shown in Fig. 1, and show the highest achieved test scores in Tab. 1. We can observe that (1) larger model sizes with a higher network capability generally benefit the achieved test scores especially on more complex games (e.g., BeamRider in Tab. 1), as larger models can achieve higher test scores under the same training time steps in most of the games as compared with the smaller vanilla-network and ResNet-14, and (2) there always exists a task-specific optimal model size where larger models cannot further improve or even degrade the test score, which we conjecture is due to the increased training difficulty associated with larger DRL agents. For instance, the vanilla network can achieve decent test scores in the Atlantis game (see Fig. 1), while ResNet-38 can only marginally improve the score with  $13.7\times$  higher FLOPs (floating-point operations). In addition, ResNet-74 performs worse than ResNet-20/38 in most of these experiments, due to its increased training difficulty within the limited training steps. We recognize that more training steps and well-tuned training hyper-parameters may help the case with ResNet-74 converge to a better optima, however the resulting inefficiency in both training and inference as compared to more efficient agents will limit the practical usability of such solutions.



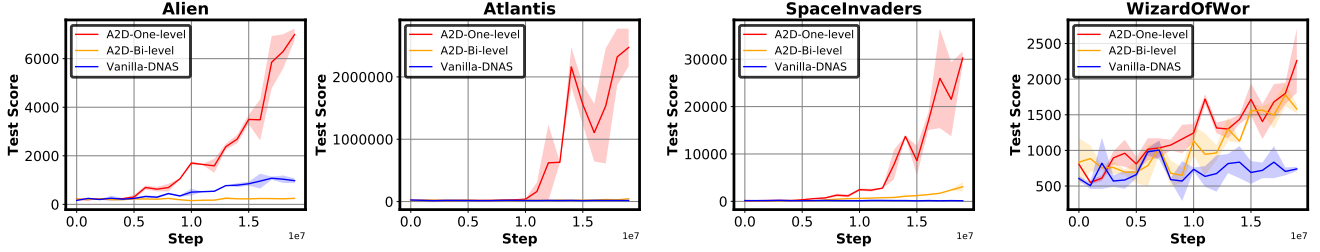


Figure 2. Test score evolution during the search processes of three different search schemes on four Atari games [4], where Vanilla-DNAS denotes directly applying NAS without distillation, and A2D-One-level and A2D-Bi-level search under the guidance of the distillation loss using one-level and bi-level optimization, respectively.

Experiments with different models on more tasks are provided in Appendix. A.

**Extracted Insights.** The above observations indicate that (1) the DNN architecture is a critical design factor in DRL despite their being under-explored in existing works, and (2) it is highly desired to design task-specific agents which optimally balance the test score and processing efficiency for different tasks. Meanwhile, manually designing dedicated agents for different tasks is time/labor-consuming, and thus not practical for addressing the growing demand for the fast development and deployment of DRL-powered intelligent solutions for numerous applications, motivating the introduction of NAS into the DRL domain to automate the design of optimal DRL agents.

## 4.2. Finding 2: Vanilla DNAS Fails in DRL

In this subsection, we present experiments and discussions to show the challenges and failures of directly applying vanilla DNAS to design DRL agents.

**Challenges of Applying DNAS to DRL.** We mainly consider DNAS [45] since its low search time and cost make it better align with our target goal of fast development and deployment of powerful and efficient DRL agents for different tasks, as compared with other NAS methods that require higher search costs and may limit the number of interactions with the environments. Different from other tasks such as visual classification that are facilitated with consistent supervision information, the training of DRL is often unstable due to the high variance in the gradient estimation as discussed in [11, 29, 1, 56], making it difficult to correctly rank the sampled networks within a limited search time. This challenge can be further exacerbated when applying DNAS to DRL, as effective DNAS requires unbiased and stable (with low variance) gradient estimation [5, 26] to guarantee the convergence while such a requirement is often not feasible in a DRL environment, especially in real-world applications.

**Evaluation Settings of Applying Vanilla DNAS.** Here we use the same search space and search settings as those for evaluating the proposed A2D framework described in Sec. 4.4 where more details can be found. In general, to evaluate the feasibility of directly applying vanilla DNAS

to DRL, we adopt the search strategy in [82] where a Gumbel Softmax [36] function is utilized to sample candidate operators from the search space and a one-level optimization to update the weight and architecture parameters with unbiased gradient estimation [26].

**Observations and Analysis.** Fig. 2 (see the blue line) visualizes the test score evolution during the search process. We can observe that the supernet can hardly converge with the consistently low rewards close to those of using random exploration among all the tasks, indicating that the supernet cannot serve as a reliable proxy to evaluate the performance of the derived networks. These observations validate our conjecture that the high variance in DRL training naturally forbids the practicality of vanilla DNAS in DRL.

## 4.3. The Proposed Distillation Mechanism

As discussed in Sec. 4.2, the key challenge of applying DNAS in DRL is the search instability caused by the high variance of the gradient estimates of DRL. Inspired by [58, 51] which show that the distillation from a teacher agent can effectively reduce the variance of gradient estimates and stabilize the training process of the student agent, we propose a distillation mechanism based on the AC-based DRL method, aiming to stabilize the NAS process and improve the optimality of the resulting DRL agents.

**Motivation.** Policy distillation [58] is one of the most natural choices thanks to both its simplicity across different tasks and its differentiable property that aligns with our goal of applying DNAS to DRL. However, vanilla policy distillation merely distills the policy without considering the value function which can play a critical role in both assisting the policy updates and reducing the variance of vanilla policy gradients. Furthermore, from the network design perspective, the value function can be viewed as a high-level semantic information on top of the extracted features which can thus provide important signals to guide the training of the feature extractor network, similar to the effect of the perceptual loss in GANs [37]. We thus hypothesize that further distilling the value function from the teacher agent can better improve the training stability and the convergence.

**Design of Our Distillation Mechanism.** We propose an AC-based distillation mechanism, where we first train an

Table 2. Benchmarking different distillation mechanisms for training the vanilla network and ResNet-14 with the guidance from a pretrained ResNet-20 on six Atari games [4], where row No.4 and No.8 are the proposed method. More results can be found in Appendix. B.

Model	No.	Distill the Actor	Reuse Teacher Critic	Distill the Critic with MSE Loss	Alien	Space- Invaders	Wizard- OfWor	Asterix	Battle- Zone	Beam- Rider
Vanilla	1				1724	1171	1320	4850	7600	5530
	2	✓			3096	26821	5560	59020	12700	14417
	3	✓	✓		249	30124	<b>6310</b>	37780	14200	15432
	<b>4 (Proposed)</b>	✓		✓	<b>3419</b>	<b>39274</b>	5960	<b>64510</b>	<b>14500</b>	<b>17806</b>
ResNet-14	5				9007	9848	2690	708500	5800	23984
	6	✓			14682	76246	<b>6300</b>	749870	16300	38311
	7	✓	✓		12674	79287	4640	695550	16400	37350
	<b>8 (Proposed)</b>	✓		✓	<b>15723</b>	<b>111189</b>	5450	<b>849400</b>	<b>18200</b>	<b>42365</b>

AC agent using a large network backbone and then guide the training of the student agent by distilling from both the actor and critic of the teacher agent. Specifically, the two distillation losses are formulated as:

$$L_{actor}^{distill} = \mathbb{E}_{\pi} \left[ \sum_{t=0}^H \pi(a_t, s_t | \theta_{\pi}^{tea}) \log \frac{\pi(a_t, s_t | \theta_{\pi}^{tea})}{\pi(a_t, s_t | \theta_{\pi}^{stu})} \right] \quad (6)$$

$$L_{critic}^{distill} = \mathbb{E}_{\pi} \left[ \sum_{t=0}^H \frac{1}{2} (V_{\pi}(s_t | \theta_v^{stu}) - V_{\pi}(s_t | \theta_v^{tea}))^2 \right] \quad (7)$$

where  $\pi(a_t, s_t | \theta_{\pi}^{tea})$  and  $\pi(a_t, s_t | \theta_{\pi}^{stu})$  are the teacher and student actor, respectively, and  $V_{\pi}(s_t | \theta_v^{tea})$  and  $V_{\pi}(s_t | \theta_v^{stu})$  are the teacher and student critic, respectively. Here we adopt KL divergence to distill the knowledge from the teacher actor following [58] and the MSE loss as a soft constraint to enforce the student critic to incorporate the estimated value of the teacher critic. Therefore, the training objective during both search and training is:

$$L_{total} = L_{policy} + L_{value} + \alpha_1 L_{entropy} + \alpha_2 L_{actor}^{distill} + \alpha_3 L_{critic}^{distill} \quad (8)$$

where  $\alpha_1$ ,  $\alpha_2$ , and  $\alpha_3$  are the weighted coefficients. As in Sec. 3, here  $L_{policy} = \mathbb{E}_{\pi} \left[ -\sum_{t=0}^H \delta_t \log(\pi(a_t, s_t | \theta_{\pi}^{stu})) \right]$  is the policy gradient loss as in [67],  $L_{value} = \mathbb{E}_{\pi} \left[ \sum_{t=0}^H \frac{1}{2} (r_t + \gamma V_{\pi}(s_{t+1} | \theta_v^{stu}) - V_{\pi}(s_t | \theta_v^{stu}))^2 \right]$  is the value loss based on the td-error [66], and  $L_{entropy} = \mathbb{E}_{\pi} \left[ \sum_{t=0}^H \pi(a_t, s_t | \theta_{\pi}^{stu}) \log(\pi(a_t, s_t | \theta_{\pi}^{stu})) \right]$  is the entropy loss on top of the policy to encourage exploration as in [24].

**Discussions about the Distillation Design.** Another choice for distilling the knowledge from the teacher critic is to directly apply the estimated value of the teacher critic as that of the student critic, i.e., without training a new student critic. However, this may lead to an overestimation of the value if the teacher critic is inaccurate as analyzed

in [72, 71, 25, 73], the resulting approximation error of which will further accumulate in the student agent. Therefore, instead of completely inheriting the teacher critic, we apply an MSE loss between the estimated value of the student and teacher critics to distill the knowledge in a soft manner, mitigating the potential of overestimation as validated in our evaluation experiments.

**Evaluation Settings.** We use the same training settings as in Sec. 4.1 except that we incorporate the distillation loss as in Eq. 8. In particular, we train a ResNet-20 model as the teacher agent for all the experiments and  $\alpha_1$ ,  $\alpha_2$ , and  $\alpha_3$  in Eq. 8 are set to be 1e-2, 1e-1, and 1e-3, respectively, in all our settings. We benchmark the proposed distillation mechanism with three baselines: (1) the original training scheme without distillation, (2) training with the distillation only from the teacher actor, i.e.,  $\alpha_3$  is zero, as in [58], and (3) training with the distillation from the teacher actor and directly reusing the estimated value from the teacher critic without training a new critic.

**Observations and Analysis.** We evaluate the proposed distillation mechanism and the three baselines by applying them to the vanilla network and ResNet-14 evaluated on six Atari games as shown in Tab. 2. We can observe that: (1) different distillation strategies generally improve the test scores compared with the ones without distillation, which is consistent with [58]; (2) Among the three distillation strategies, our proposed distillation mechanism consistently outperforms the other two strategies in achieving higher test scores on most of tasks, and (3) reusing the teacher critic combined with the distillation from the teacher actor (i.e., row No.3 and No.7 in Tab. 2) suffers from negative effects in six out of the 12 cases compared with the case of only distilling the actor, verifying that our hypothesized overestimation problem can occur if merely inheriting the teacher critic without training a student critic.

More benchmark experiments over the SOTA policy distillation [58] are provided in Appendix. B.

#### 4.4. The Proposed A2D Framework

In this subsection, we describe our A2D framework, which to our best knowledge is the first NAS framework for

DRL and makes use of the distillation mechanism presented in Sec. 4.3. Specifically, A2D integrates the knowledge distilled from a teacher agent to stabilize the search process of NAS and adopts DNAS considering its advantageous search efficiency following [45, 80], which can be formulated as a one-level optimization problem:

$$\min_{\theta_\pi, \theta_v, \alpha} L_{total}(\theta_\pi, \theta_v, \alpha) + \lambda L_{cost}(\alpha) \quad (9)$$

where  $L_{total}$  is the distillation-based loss (see Eq. 8),  $L_{cost}$  is an efficiency loss (e.g., the total number of floating-point operations (FLOPs)) weighted by the coefficient  $\lambda$  and determined by the searched network architecture, and  $\alpha$  is the architecture parameter which stores the probability of each candidate operator.

**Optimization Method of A2D.** As shown in Eq. 9, We adopt a one-level optimization in A2D, i.e., update the weight and architecture parameters in the same iteration as in [82], instead of using a bi-level optimization as in [45]. Our consideration is that the bi-level optimization induces biased gradient estimation due to the approximation resulting from its one-step stochastic gradient descent [26, 5], which may harm the search stability especially in the DRL context. In contrast, the one-level optimization has unbiased gradient estimation [26] and its potential over-fitting problem can be alleviated by the randomness introduced by the Gumbel Softmax function [36] as widely adopted in [82, 34, 6]. We will benchmark these two optimization methods in the experiments.

**The NAS Sampling Method.** During the DNAS search, each layer in the supernet is formulated as a weighted sum of the outputs from all the  $N$  candidate operators, i.e.,

$$A^{l+1} = \sum_{i=1}^N GS(\alpha_i^l) O_i^l(A^l) \quad (10)$$

$$\text{where } GS(\alpha_i^l) = \frac{\exp[(\log(\alpha_i^l) + g_i^l)/\tau]}{\sum_i \exp[(\log(\alpha_i^l) + g_i^l)/\tau]} \quad (11)$$

where  $A^l$  and  $A^{l+1}$  are the output activations of two consecutive layers, respectively;  $O_i^l$  is the  $i$ -th candidate operator in the  $l$ -th layer whose probability is controlled by  $\alpha_i^l$ ;  $GS$  is the Gumbel Softmax function [36] which relaxes the discrete architecture distribution to be continuous and differentiable using the reparameterization trick;  $g_i^l$  is a random variable sampled from the Gumbel distribution; and  $\tau$  is a temperature parameter which is annealing during the search process to enforce  $GS(\alpha_i^l)$  to be close to an one-hot vector at the end of search for narrowing the gap between the supernet and the derived network.

The search algorithm of A2D is summarized in Alg. 1.

---

**Algorithm 1** Auto-Agent Distiller (A2D): Searching for Efficient DRL Agents

---

**Require:** the total steps  $T_{max}$ , the rollout length  $L$ , the discount factor  $\gamma$ , the teacher actor and critic  $\pi(\cdot|\theta_\pi^{tea})$  and  $V_\pi(\cdot|\theta_v^{tea})$ , the learning rates of supernet weights and architecture parameters  $\eta_1$  and  $\eta_2$ , respectively, the weight of efficiency loss  $\lambda$   
Initialize  $\pi(\cdot|\theta_\pi^{stu})$ ,  $V_\pi(\cdot|\theta_v^{stu})$  and the architecture  $\alpha$   
Initialize the step counter  $t \leftarrow 1$   
**repeat**  
   $t_{start} = t$   
  Get state  $s_t$   
  **repeat**  
    Perform  $a_t \sim \pi(a_t, s_t|\theta_\pi^{stu})$  based on Eq. 10 and Eq. 11  
    Receive reward  $r_t$  and new state  $s_{t+1}$   
     $t \leftarrow t + 1$   
  **until** terminal  $s_t$  **or**  $t - t_{start} == L$   
  **for**  $i \in \{t_{start}, \dots, t - 1\}$  **do**  
     $\delta_t = r_t + \gamma V_\pi(s_{t+1}|\theta_v^{stu}) - V_\pi(s_t|\theta_v^{stu})$   
    Calculate  $L_{total}$  in Eq. 8 based on  $\delta_t$ ,  $\pi(a_t, s_t|\theta_\pi^{tea})$ , and  $V_\pi(s_t|\theta_v^{tea})$   
    Update  $\theta_\pi^{stu}$ :  $\theta_\pi^{stu} \leftarrow \theta_\pi^{stu} - \eta_1 \nabla_{\theta_\pi^{stu}} L_{total}$   
    Update  $\theta_v^{stu}$ :  $\theta_v^{stu} \leftarrow \theta_v^{stu} - \eta_1 \nabla_{\theta_v^{stu}} L_{total}$   
    Update  $\alpha$ :  $\alpha \leftarrow \alpha - \eta_2 \nabla_\alpha (L_{total} + \lambda L_{cost})$   
  **end for**  
**until**  $t > T_{max}$   
Derive the final agent with the highest  $\alpha$   
**return** the final agent

---

**Evaluation settings.** Search space: the supernet structure follows the network design in Sec. 4.1 with a searchable feature extractor and two light-weight headers served as the actor and critic, respectively. Specifically, we adopt a sequential block-based supernet structure as [80] for facilitating hardware efficiency, which includes 14 searchable cells with each containing 9 candidate operators, leading to a search space of  $9^{14}$  choices. More details about the supernet structure are provided in Appendix. D. Search settings: we update the architecture parameters using an Adam optimizer with a momentum of 0.9 and a fixed learning rate of  $1e-3$ . The initial temperature  $\tau$  in Eq. 11 is set to 5 and decayed by 0.98 every  $1e5$  steps to ensure the final temperature to be close to 0.1. The training settings of the weights and the objective function are the same as in Sec. 4.3 except that we only search for  $2e7$  steps for an acceptable search time. Derive the final agent: we select the operators with the highest probability indicated by  $\alpha$  to derive the searched agent, and then train it from scratch with the proposed distillation mechanism following the training setting in Sec. 4.3 under the guidance of a pretrain ResNet-20 agent.

**Observations and Analysis.** Test score evolution during search: we visualize the test score evolution searched using both the one-level and bi-level optimization, respectively, with both under the guidance of the distillation loss, as shown in Fig. 2. We can observe that the test scores

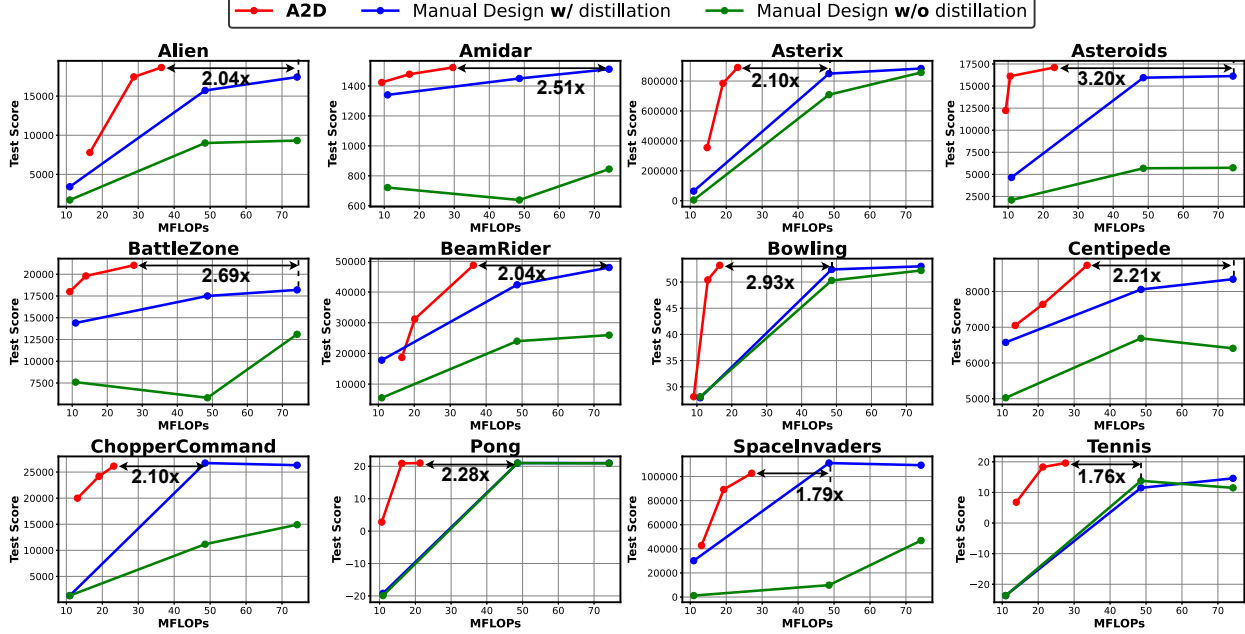


Figure 3. Test score and efficiency trade-offs achieved by our A2D and the manually designed DRL on 12 Atari games [4], where the three manual designs use the vanilla network, ResNet-14, and ResNet-20 introduced in Sec. 4.1.

remain low when searching with the bi-level optimization, validating our mentioned hypothesis that the supernet cannot serve as an accurate proxy to indicate the performance of the sampled subnetworks. In contrast, searching with the one-level optimization leads to a consistent improvement in the test scores during search, demonstrating the first framework that successfully makes NAS possible in DRL.

**Test score vs. efficiency trade-offs on 12 Atari games:** Fig. 3 shows the test score and efficiency trade-offs of both the networks searched by the proposed A2D and the manual designs trained w/ and w/o the proposed distillation mechanism, the latter of which includes the vanilla network, ResNet-14, and ResNet-20 as introduced in Sec. 4.1. We can observe that (1) our A2D framework achieves comparable test scores with the best baseline at the cost of  $1.76\times \sim 3.20\times$  fewer FLOPs, and (2) the proposed A2D can derive DRL agents with different model sizes to automatically adapt to the task difficulty, e.g., fewer than 20 MFLOPs for the Bowling game and near 40 MFLOPs for the Alien game as shown in Fig. 3, verifying that A2D is capable to identify the optimal agent model sizes depending on the target tasks to maximize both the test score and processing efficiency. Although the vanilla network is also promising in terms of the required FLOPs, it requires a larger parameter number, e.g.,  $5.83\times$  compared with ResNet-20, and more than  $10\times$  larger than the searched networks of A2D.

**Discussions.** Our A2D framework is to study the practicality and possibility of applying DNAS to search for DRL agents. While the above experiments consistently validate its effectiveness over manually expert-designed DRL

agents, we recognize that A2D is merely one very first step towards automated design of DRL agents. Many further explorations can be performed on top of A2D, including the exploration of (1) larger and more complex search spaces, (2) different DRL recipes (e.g., on-policy/off-policy), (3) transferability to other DRL algorithms, and (4) the extension to real-world applications (e.g., autonomous driving), which we leave for our future work.

## 5. Conclusion

The recent breakthroughs of DRL agents have motivated a growing demand for deploying DRL agents into intelligent devices for real-time control while the prohibitive computational cost of DRL stands at the odds with the limited on-device resources. To close this gap, we first identify that there exists a task-specific optimal model size that maximizes both the test scores and efficiency, and then propose the A2D framework, which to our best knowledge is the first NAS applied to DRL to automatically search for the optimal DRL agents for various tasks based on a novel distillation mechanism to stabilize the notorious searching process and improve optimality. Extensive experiments and ablation studies consistently validate the superiority of the proposed A2D framework over manually expert-designed DRL in optimizing the test scores and processing efficiency. This work enhances our understanding in NAS for DRL and can open up the possibility of automated and fast development of DRL-powered solutions for real-world applications.



## References

- [1] Kai Arulkumaran, Marc Peter Deisenroth, Miles Brundage, and Anil Anthony Bharath. Deep reinforcement learning: A brief survey. *IEEE Signal Processing Magazine*, 34(6):26–38, 2017. 2, 3, 5
- [2] Gabriel Barth-Maron, Matthew W Hoffman, David Budden, Will Dabney, Dan Horgan, Dhruva Tb, Alistair Muldal, Nicolas Heess, and Timothy Lillicrap. Distributed distributional deterministic policy gradients. *arXiv preprint arXiv:1804.08617*, 2018. 2
- [3] Marc G Bellemare, Will Dabney, and Rémi Munos. A distributional perspective on reinforcement learning. *arXiv preprint arXiv:1707.06887*, 2017. 2
- [4] Marc G Bellemare, Yavar Naddaf, Joel Veness, and Michael Bowling. The arcade learning environment: An evaluation platform for general agents. *Journal of Artificial Intelligence Research*, 47:253–279, 2013. 4, 5, 6, 8
- [5] Kaifeng Bi, Changping Hu, Lingxi Xie, Xin Chen, Longhui Wei, and Qi Tian. Stabilizing darts with amended gradient estimation on architectural parameters. *arXiv preprint arXiv:1910.11831*, 2019. 5, 7
- [6] Kaifeng Bi, Lingxi Xie, Xin Chen, Longhui Wei, and Qi Tian. Gold-nas: Gradual, one-level, differentiable. *arXiv preprint arXiv:2007.03331*, 2020. 7
- [7] Tim Brys, Anna Harutyunyan, Matthew E Taylor, and Ann Nowé. Policy transfer using reward shaping. In *Proceedings of the 2015 International Conference on Autonomous Agents and Multiagent Systems*, pages 181–188, 2015. 2
- [8] Han Cai, Ligeng Zhu, and Song Han. Proxylessnas: Direct neural architecture search on target task and hardware. *arXiv preprint arXiv:1812.00332*, 2018. 3
- [9] Daoyuan Chen, Yaliang Li, Minghui Qiu, Zhen Wang, Bofang Li, Bolin Ding, Hongbo Deng, Jun Huang, Wei Lin, and Jingren Zhou. Adabert: Task-adaptive bert compression with differentiable neural architecture search. *arXiv preprint arXiv:2001.04246*, 2020. 3
- [10] Wuyang Chen, Xinyu Gong, Xianming Liu, Qian Zhang, Yuan Li, and Zhangyang Wang. Fasterseg: Searching for faster real-time semantic segmentation. *arXiv preprint arXiv:1912.10917*, 2019. 3
- [11] Richard Cheng, Abhinav Verma, Gabor Orosz, Swarat Chaudhuri, Yisong Yue, and Joel W Burdick. Control regularization for reduced variance reinforcement learning. *arXiv preprint arXiv:1905.05380*, 2019. 2, 3, 5
- [12] Paul Covington, Jay Adams, and Emre Sargin. Deep neural networks for youtube recommendations. In *Proceedings of the 10th ACM Conference on Recommender Systems*, New York, NY, USA, 2016. 1
- [13] Giuseppe Cuccu, Matthew Luci, Jürgen Schmidhuber, and Faustino Gomez. Intrinsically motivated neuroevolution for vision-based reinforcement learning. In *2011 IEEE International Conference on Development and Learning (ICDL)*, volume 2, pages 1–7. IEEE, 2011. 2
- [14] Wojciech Marian Czarnecki, Razvan Pascanu, Simon Osindero, Siddhant M Jayakumar, Grzegorz Swirszcz, and Max Jaderberg. Distilling policy distillation. *arXiv preprint arXiv:1902.02186*, 2019. 2
- [15] Y. Deng, F. Bao, Y. Kong, Z. Ren, and Q. Dai. Deep direct reinforcement learning for financial signal representation and trading. *IEEE Transactions on Neural Networks and Learning Systems*, 28(3):653–664, 2017. 1
- [16] Sam Michael Devlin and Daniel Kudenko. Dynamic potential-based reward shaping. In *Proceedings of the 11th International Conference on Autonomous Agents and Multi-agent Systems*, pages 433–440. IFAAMAS, 2012. 2
- [17] Lasse Espeholt, Hubert Soyer, Remi Munos, Karen Simonyan, Volodymyr Mnih, Tom Ward, Yotam Doron, Vlad Firoiu, Tim Harley, Iain Dunning, et al. Impala: Scalable distributed deep-rl with importance weighted actor-learner architectures. *arXiv preprint arXiv:1802.01561*, 2018. 2, 4, 12
- [18] Meire Fortunato, Mohammad Gheshlaghi Azar, Bilal Piot, Jacob Menick, Ian Osband, Alex Graves, Vlad Mnih, Remi Munos, Demis Hassabis, Olivier Pietquin, et al. Noisy networks for exploration. *arXiv preprint arXiv:1706.10295*, 2017. 2
- [19] Vincent François-Lavet. *Contributions to deep reinforcement learning and its applications in smartgrids*. PhD thesis, Université de Liège, Liège, Belgique, Sept. 2017. 1
- [20] Yonggan Fu, Wuyang Chen, Haotao Wang, Haoran Li, Yingyan Lin, and Zhangyang Wang. Autogan-distiller: Searching to compress generative adversarial networks. *arXiv preprint arXiv:2006.08198*, 2020. 3
- [21] Scott Fujimoto, Herke Van Hoof, and David Meger. Addressing function approximation error in actor-critic methods. *arXiv preprint arXiv:1802.09477*, 2018. 2
- [22] D. Gandhi, L. Pinto, and A. Gupta. Learning to fly by crashing. In *2017 IEEE/RSJ International Conference on Intelligent Robots and Systems (IROS)*, pages 3948–3955, 2017. 1
- [23] Faustino Gomez and Jürgen Schmidhuber. Evolving modular fast-weight networks for control. In *International Conference on Artificial Neural Networks*, pages 383–389. Springer, 2005. 2
- [24] Tuomas Haarnoja, Aurick Zhou, Pieter Abbeel, and Sergey Levine. Soft actor-critic: Off-policy maximum entropy deep reinforcement learning with a stochastic actor. *arXiv preprint arXiv:1801.01290*, 2018. 2, 4, 6
- [25] Hado Hasselt. Double q-learning. *Advances in neural information processing systems*, 23:2613–2621, 2010. 6
- [26] Chaoyang He, Haishan Ye, Li Shen, and Tong Zhang. Mile-nas: Efficient neural architecture search via mixed-level reformulation. In *Proceedings of the IEEE/CVF Conference on Computer Vision and Pattern Recognition*, pages 11993–12002, 2020. 5, 7
- [27] Kaiming He, Xiangyu Zhang, Shaoqing Ren, and Jian Sun. Deep residual learning for image recognition. In *Proceedings of the IEEE conference on computer vision and pattern recognition*, pages 770–778, 2016. 4
- [28] Kaiming He, Xiangyu Zhang, Shaoqing Ren, and Jian Sun. Identity mappings in deep residual networks. In *European conference on computer vision*, pages 630–645. Springer, 2016. 4, 12

- [29] Peter Henderson, Riashat Islam, Philip Bachman, Joelle Pineau, Doina Precup, and David Meger. Deep reinforcement learning that matters. *arXiv preprint arXiv:1709.06560*, 2017. 2, 3, 5
- [30] Matteo Hessel, Joseph Modayil, Hado Van Hasselt, Tom Schaul, Georg Ostrovski, Will Dabney, Dan Horgan, Bilal Piot, Mohammad Azar, and David Silver. Rainbow: Combining improvements in deep reinforcement learning. *arXiv preprint arXiv:1710.02298*, 2017. 2
- [31] Todd Hester, Matej Vecerik, Olivier Pietquin, Marc Lanctot, Tom Schaul, Bilal Piot, Dan Horgan, John Quan, Andrew Sendonaris, Gabriel Dulac-Arnold, et al. Deep q-learning from demonstrations. *arXiv preprint arXiv:1704.03732*, 2017. 2
- [32] Geoffrey Hinton, Oriol Vinyals, and Jeff Dean. Distilling the knowledge in a neural network. *arXiv preprint arXiv:1503.02531*, 2015. 2
- [33] Andrew Howard, Mark Sandler, Grace Chu, Liang-Chieh Chen, Bo Chen, Mingxing Tan, Weijun Wang, Yukun Zhu, Ruoming Pang, Vijay Vasudevan, et al. Searching for mobilenetv3. In *Proceedings of the IEEE International Conference on Computer Vision*, pages 1314–1324, 2019. 3
- [34] Shoukang Hu, Sirui Xie, Hehui Zheng, Chunxiao Liu, Jianping Shi, Xunying Liu, and Dahua Lin. Dsnas: Direct neural architecture search without parameter retraining. In *Proceedings of the IEEE/CVF Conference on Computer Vision and Pattern Recognition*, pages 12084–12092, 2020. 7
- [35] Frank Hutter, Lars Kotthoff, and Joaquin Vanschoren. *Automated machine learning: methods, systems, challenges*. Springer Nature, 2019. 2
- [36] Eric Jang, Shixiang Gu, and Ben Poole. Categorical reparameterization with gumbel-softmax. *arXiv preprint arXiv:1611.01144*, 2016. 5, 7
- [37] Justin Johnson, Alexandre Alahi, and Li Fei-Fei. Perceptual losses for real-time style transfer and super-resolution. In *European conference on computer vision*, pages 694–711. Springer, 2016. 5
- [38] Bingyi Kang, Zequn Jie, and Jiashi Feng. Policy optimization with demonstrations. In *International Conference on Machine Learning*, pages 2469–2478, 2018. 2
- [39] Beomjoon Kim, Amir-massoud Farahmand, Joelle Pineau, and Doina Precup. Learning from limited demonstrations. In *Advances in Neural Information Processing Systems*, pages 2859–2867, 2013. 2
- [40] Vijay R Konda and John N Tsitsiklis. Actor-critic algorithms. In *Advances in neural information processing systems*, pages 1008–1014, 2000. 2, 3, 4
- [41] Royson Lee, Łukasz Dudziak, Mohamed Abdelfattah, Stylianos I Venieris, Hyeji Kim, Hongkai Wen, and Nicholas D Lane. Journey towards tiny perceptual super-resolution. *arXiv preprint arXiv:2007.04356*, 2020. 3
- [42] Sergey Levine, Chelsea Finn, Trevor Darrell, and Pieter Abbeel. End-to-end training of deep visuomotor policies. *J. Mach. Learn. Res.*, 17(1):1334–1373, Jan. 2016. 1
- [43] Timothy P Lillicrap, Jonathan J Hunt, Alexander Pritzel, Nicolas Heess, Tom Erez, Yuval Tassa, David Silver, and Daan Wierstra. Continuous control with deep reinforcement learning. *arXiv preprint arXiv:1509.02971*, 2015. 2
- [44] Chenxi Liu, Liang-Chieh Chen, Florian Schroff, Hartwig Adam, Wei Hua, Alan L Yuille, and Li Fei-Fei. Auto-deeplab: Hierarchical neural architecture search for semantic image segmentation. In *Proceedings of the IEEE conference on computer vision and pattern recognition*, pages 82–92, 2019. 3
- [45] Hanxiao Liu, Karen Simonyan, and Yiming Yang. Darts: Differentiable architecture search. *arXiv preprint arXiv:1806.09055*, 2018. 2, 3, 5, 7
- [46] Yang Liu, Prajit Ramachandran, Qiang Liu, and Jian Peng. Stein variational policy gradient. *arXiv preprint arXiv:1704.02399*, 2017. 2
- [47] Volodymyr Mnih, Adria Puigdomenech Badia, Mehdi Mirza, Alex Graves, Timothy Lillicrap, Tim Harley, David Silver, and Koray Kavukcuoglu. Asynchronous methods for deep reinforcement learning. In *International conference on machine learning*, pages 1928–1937, 2016. 2, 4, 12
- [48] Volodymyr Mnih, Koray Kavukcuoglu, David Silver, Andrei A Rusu, Joel Veness, Marc G Bellemare, Alex Graves, Martin Riedmiller, Andreas K Fiedland, Georg Ostrovski, et al. Human-level control through deep reinforcement learning. *nature*, 518(7540):529–533, 2015. 1, 2, 4
- [49] Ashvin Nair, Bob McGrew, Marcin Andrychowicz, Wojciech Zaremba, and Pieter Abbeel. Overcoming exploration in reinforcement learning with demonstrations. In *2018 IEEE International Conference on Robotics and Automation (ICRA)*, pages 6292–6299. IEEE, 2018. 2
- [50] Andrew Y Ng, Daishi Harada, and Stuart Russell. Policy invariance under reward transformations: Theory and application to reward shaping. In *ICML*, volume 99, pages 278–287, 1999. 2
- [51] Emilio Parisotto, Jimmy Lei Ba, and Ruslan Salakhutdinov. Actor-mimic: Deep multitask and transfer reinforcement learning. *arXiv preprint arXiv:1511.06342*, 2015. 2, 5
- [52] Hieu Pham, Melody Y Guan, Barret Zoph, Quoc V Le, and Jeff Dean. Efficient neural architecture search via parameter sharing. *arXiv preprint arXiv:1802.03268*, 2018. 3
- [53] Lerrel Pinto, Marcin Andrychowicz, Peter Welinder, Wojciech Zaremba, and Pieter Abbeel. Asymmetric actor critic for image-based robot learning. 06 2018. 1
- [54] Antonio Polino, Razvan Pascanu, and Dan Alistarh. Model compression via distillation and quantization. *arXiv preprint arXiv:1802.05668*, 2018. 2
- [55] Esteban Real, Alok Aggarwal, Yanping Huang, and Quoc V Le. Regularized evolution for image classifier architecture search. In *Proceedings of the aaai conference on artificial intelligence*, volume 33, pages 4780–4789, 2019. 3
- [56] Benjamin Recht. A tour of reinforcement learning: The view from continuous control. *Annual Review of Control, Robotics, and Autonomous Systems*, 2:253–279, 2019. 2, 3, 5
- [57] Gavin A Rummery and Mahesan Niranjana. *On-line Q-learning using connectionist systems*, volume 37. University of Cambridge, Department of Engineering Cambridge, UK, 1994. 2

- [58] Andrei A Rusu, Sergio Gomez Colmenarejo, Caglar Gulcehre, Guillaume Desjardins, James Kirkpatrick, Razvan Pascanu, Volodymyr Mnih, Koray Kavukcuoglu, and Raia Hadsell. Policy distillation. *arXiv preprint arXiv:1511.06295*, 2015. 2, 5, 6, 12, 13
- [59] Stefan Schaal. Learning from demonstration. In *Advances in neural information processing systems*, pages 1040–1046, 1997. 2
- [60] Tom Schaul, John Quan, Ioannis Antonoglou, and David Silver. Prioritized experience replay. *arXiv preprint arXiv:1511.05952*, 2015. 2
- [61] Simon Schmitt, Jonathan J Hudson, Augustin Zidek, Simon Osindero, Carl Doersch, Wojciech M Czarnecki, Joel Z Leibo, Heinrich Kuttler, Andrew Zisserman, Karen Simonyan, et al. Kickstarting deep reinforcement learning. *arXiv preprint arXiv:1803.03835*, 2018. 2
- [62] John Schulman, Sergey Levine, Pieter Abbeel, Michael Jordan, and Philipp Moritz. Trust region policy optimization. In *International conference on machine learning*, pages 1889–1897, 2015. 2
- [63] John Schulman, Filip Wolski, Prafulla Dhariwal, Alec Radford, and Oleg Klimov. Proximal policy optimization algorithms. *arXiv preprint arXiv:1707.06347*, 2017. 2
- [64] David Silver, Guy Lever, Nicolas Heess, Thomas Degris, Daan Wierstra, and Martin Riedmiller. Deterministic policy gradient algorithms. 2014. 2
- [65] Dimitrios Stamoulis, Ruizhou Ding, Di Wang, Dimitrios Lymberopoulos, Bodhi Priyantha, Jie Liu, and Diana Marculescu. Single-path nas: Designing hardware-efficient convnets in less than 4 hours. In *Joint European Conference on Machine Learning and Knowledge Discovery in Databases*, pages 481–497. Springer, 2019. 3
- [66] Richard S Sutton. Learning to predict by the methods of temporal differences. *Machine learning*, 3(1):9–44, 1988. 3, 6
- [67] Richard S Sutton, David A McAllester, Satinder P Singh, and Yishay Mansour. Policy gradient methods for reinforcement learning with function approximation. In *Advances in neural information processing systems*, pages 1057–1063, 2000. 2, 3, 6
- [68] Mingxing Tan, Bo Chen, Ruoming Pang, Vijay Vasudevan, Mark Sandler, Andrew Howard, and Quoc V Le. Mnasnet: Platform-aware neural architecture search for mobile. In *Proceedings of the IEEE Conference on Computer Vision and Pattern Recognition*, pages 2820–2828, 2019. 3
- [69] Mingxing Tan and Quoc V Le. Efficientnet: Rethinking model scaling for convolutional neural networks. *arXiv preprint arXiv:1905.11946*, 2019. 1, 3
- [70] Yee Teh, Victor Bapst, Wojciech M Czarnecki, John Quan, James Kirkpatrick, Raia Hadsell, Nicolas Heess, and Razvan Pascanu. Distral: Robust multitask reinforcement learning. In *Advances in Neural Information Processing Systems*, pages 4496–4506, 2017. 2
- [71] Sebastian Thrun and Anton Schwartz. Issues in using function approximation for reinforcement learning. In *Proceedings of the 1993 Connectionist Models Summer School Hillsdale, NJ. Lawrence Erlbaum*, 1993. 6
- [72] Hado Van Hasselt, Arthur Guez, and David Silver. Deep reinforcement learning with double q-learning. *arXiv preprint arXiv:1509.06461*, 2015. 2, 6
- [73] Hado Philip van Hasselt. *Insights in reinforcement learning*. Hado van Hasselt, 2011. 6
- [74] Mel Vecerik, Todd Hester, Jonathan Scholz, Fumin Wang, Olivier Pietquin, Bilal Piot, Nicolas Heess, Thomas Rothörl, Thomas Lampe, and Martin Riedmiller. Leveraging demonstrations for deep reinforcement learning on robotics problems with sparse rewards. *arXiv preprint arXiv:1707.08817*, 2017. 2
- [75] Alvin Wan, Xiaoliang Dai, Peizhao Zhang, Zijian He, Yuan-dong Tian, Saining Xie, Bichen Wu, Matthew Yu, Tao Xu, Kan Chen, et al. Fbnetv2: Differentiable neural architecture search for spatial and channel dimensions. In *Proceedings of the IEEE/CVF Conference on Computer Vision and Pattern Recognition*, pages 12965–12974, 2020. 3
- [76] Ziyu Wang, Victor Bapst, Nicolas Heess, Volodymyr Mnih, Remi Munos, Koray Kavukcuoglu, and Nando de Freitas. Sample efficient actor-critic with experience replay. *arXiv preprint arXiv:1611.01224*, 2016. 2
- [77] Ziyu Wang, Tom Schaul, Matteo Hessel, Hado Hasselt, Marc Lanctot, and Nando Freitas. Dueling network architectures for deep reinforcement learning. In *International conference on machine learning*, pages 1995–2003, 2016. 2
- [78] Christopher JCH Watkins and Peter Dayan. Q-learning. *Machine learning*, 8(3-4):279–292, 1992. 2
- [79] Eric Wiewiora, Garrison W Cottrell, and Charles Elkan. Principled methods for advising reinforcement learning agents. In *Proceedings of the 20th International Conference on Machine Learning (ICML-03)*, pages 792–799, 2003. 2
- [80] Bichen Wu, Xiaoliang Dai, Peizhao Zhang, Yanghan Wang, Fei Sun, Yiming Wu, Yuandong Tian, Peter Vajda, Yangqing Jia, and Kurt Keutzer. Fbnet: Hardware-aware efficient convnet design via differentiable neural architecture search. In *Proceedings of the IEEE Conference on Computer Vision and Pattern Recognition*, pages 10734–10742, 2019. 3, 7, 12
- [81] Yuhuai Wu, Elman Mansimov, Roger B Grosse, Shun Liao, and Jimmy Ba. Scalable trust-region method for deep reinforcement learning using kronecker-factored approximation. In *Advances in neural information processing systems*, pages 5279–5288, 2017. 2
- [82] Sirui Xie, Hehui Zheng, Chunxiao Liu, and Liang Lin. Snas: stochastic neural architecture search. *arXiv preprint arXiv:1812.09926*, 2018. 3, 5, 7
- [83] Yurong You, Xinlei Pan, Ziyang Wang, and Cewu Lu. Virtual to real reinforcement learning for autonomous driving. *CoRR*, abs/1704.03952, 2017. 1
- [84] Xiaoqin Zhang and Huimin Ma. Pretraining deep actor-critic reinforcement learning algorithms with expert demonstrations. *CoRR*, abs/1801.10459, 2018. 2
- [85] Zhuangdi Zhu, Kaixiang Lin, and Jiayu Zhou. Transfer learning in deep reinforcement learning: A survey. *arXiv preprint arXiv:2009.07888*, 2020. 2
- [86] Barret Zoph and Quoc V Le. Neural architecture search with reinforcement learning. *arXiv preprint arXiv:1611.01578*, 2016. 2, 3

- [87] Barret Zoph, Vijay Vasudevan, Jonathon Shlens, and Quoc V Le. Learning transferable architectures for scalable image recognition. In *Proceedings of the IEEE conference on computer vision and pattern recognition*, pages 8697–8710, 2018. 2, 3

## A. Evaluation of the scalability with model sizes on more tasks

We evaluate the scalability of DRL with different model sizes on more tasks to better support the analysis in Sec. 4.1. As shown in Tab. 3, we can draw observations consistent with Sec. 4.1 that (1) larger model sizes with a higher network capability generally benefit the achieved test scores especially on more complex games, and (2) there exists a task-specific optimal model size where larger models cannot further improve or even degrade the test score, which motivates the task-specific agent design.

Table 3. The best test scores achieved by different models on more Atari games.

Atari Games	Vanilla	ResNet-14	ResNet-20	ResNet-38	ResNet-74
Breakout	523.7	776.5	811	<b>818.5</b>	2.2
Alien	1724	9007	<b>9323</b>	8829	4456
Asterix	4850	708500	<b>856800</b>	756120	539060
Atlantis	3064320	3127390	3156130	<b>3181090</b>	3046490
TimePilot	4780	9070	<b>9680</b>	9500	9040
SpaceInvaders	1171	9848	<b>46870</b>	17962	15111
WizardOfWor	1320	2690	<b>3580</b>	3160	1850
Qbert	15085	13587	12385	<b>15577.5</b>	14097
Pong	-19.9	<b>21.0</b>	20.9	20.9	20.8
Tennis	-23.7	13.8	11.5	<b>19.6</b>	19.3
Amidar	721.8	638.6	<b>845.2</b>	138.3	493.9
Asteroids	2095	5690	<b>5744</b>	1947	4792
Assault	10164	14470	<b>17314</b>	12406.5	9849
BankHeist	1152	<b>1288</b>	1284	981	1163
BattleZone	7600	5800	13100	<b>13300</b>	4100
BeamRider	5530	23984	25961	29498	<b>30048</b>
Bowling	28.1	53	<b>59.2</b>	33.2	50.8
Boxing	4.2	<b>100</b>	<b>100</b>	99.3	87.1
Centipede	5025	6690	6410	6384.6	<b>6899</b>
ChopperCommand	1320	11170	<b>14910</b>	4370	8240
CrazyClimber	118300	128710	129550	130620	<b>132720</b>
DemonAttack	318349	481818	484382	<b>494569</b>	448450
Gopher	11914	<b>63926</b>	51112	42720	15340
Gravitar	475	565	490	<b>660</b>	490
Jamesbond	515	570	575	<b>640</b>	580
Kangaroo	160	<b>8950</b>	120	120	140
Krull	9412	<b>9466.2</b>	7020	7360.2	9192.3
KungFuMaster	<b>35830</b>	35450	34390	34750	34240
MsPacman	2712	4541	<b>5853</b>	3676	2556
NameThisGame	5808	17784	<b>18908</b>	18135	14409
PrivateEye	<b>100</b>	<b>100</b>	<b>100</b>	<b>100</b>	<b>100</b>
Riverraid	9164	<b>31757</b>	29037	27146	23521

## B. Evaluation of the proposed distillation mechanism on more tasks

To further validate the proposed distillation mechanism in Sec. 4.3, we benchmark the proposed distillation mechanism with the SOTA policy distillation method [58] for training the vanilla network and ResNet-14 on more tasks as shown in Tab. 4. We can observe that our proposed distillation achieves higher test scores in 26 out of the total 32 cases and comparable test scores in the remaining cases, verify-

ing the superiority of distilling both the actor and critic as analyzed in Sec. 4.3.

## C. ResNet-based network structure

The overall network design follows existing AC-based DRL methods [17, 47], which use a heavy feature extractor and two light-headers (implemented using two fully-connected layers) to design the actor and critic, respectively. For the feature extractor part, we follow the ResNet structure for CIFAR-10 dataset in [28] with two modifications: (1) we modify the stride of the first convolution to be two in order to adapt to the  $84 \times 84$  input resolutions of Atari games, and (2) we modify the output dimension of the final fully-connected layer to be 256, which serves as the input to the actor and critic headers.

## D. A2D’s search space

The supernet structure of A2D follows the #groups, #channels, and stride settings as the ResNet-like manual network design in Appendix. C. In particular, the supernet contains three groups with 5, 4, 5 searchable blocks respectively and all the blocks within the same group share the same basic channel numbers. Inspired by FBNet [80], we have nine candidate operations for each searchable block: standard convolutions with a kernel size 3/5, inverted residual blocks with a kernel size 3/5, a channel expansion of 1/3/5, and skip connections, leading to a search space of  $9^{14}$  choices.



Table 4. Benchmark the proposed distillation mechanism with (1) training without distillation, and (2) training with policy distillation [58] without distilling the critic.

Atari Games	Vanilla			ResNet-14		
	No distillation	Policy distillation [58]	The proposed distillation	No distillation	Policy distillation [58]	The proposed distillation
Atlantis	3064320	3159240	<b>3160470</b>	3127390	2845630	<b>3148450</b>
Alien	1724	3096	<b>3419</b>	9007	14682	<b>15723</b>
TimePilot	4780	9800	<b>10200</b>	9070	10490	<b>10510</b>
SpaceInvaders	1171	26821	<b>39274</b>	9848	76246	<b>111189</b>
WizardOfWor	1320	<b>6310</b>	5960	2690	<b>6300</b>	5450
Asterix	4850	59020	<b>64510</b>	708500	749870	<b>849400</b>
Qbert	15085	<b>15687.5</b>	15625	13587	<b>17980</b>	15470
Amidar	721.8	<b>1452.5</b>	1340.6	638.6	1439	<b>1450.2</b>
Asteroids	2095	4131	<b>4647</b>	5690	15371	<b>15947</b>
BattleZone	7600	12700	<b>14500</b>	5800	16300	<b>18200</b>
BeamRider	5530	14417	<b>17806</b>	23984	38311	<b>42365</b>
Boxing	4.2	2.8	<b>100</b>	<b>100</b>	<b>100</b>	<b>100</b>
Centipede	5025	5800	<b>6575.5</b>	6690	7744.3	<b>8056.9</b>
ChopperCommand	1320	15900	<b>19120</b>	11170	26320	<b>31190</b>
CrazyClimber	118300	138610	<b>145700</b>	128710	135290	<b>138470</b>
DemonAttack	318349	463823	<b>483490</b>	481818	517801	<b>521051</b>